# Abstract

We present a comprehensive discussion on the self-assembly mechanisms and domain coarsening of phase segregation when a homogeneously mixed state is quenched from a high temperature to below the critical temperature. We utilized the dissipative particle dynamics (DPD) simulation method in $d = 3$. We explored the growth law for various systems, including simple and polymeric fluids such as polymer melts and blends. Moreover, we also examined the effect of external stimuli on the evolution morphology and dynamical scaling of polymeric fluid systems.

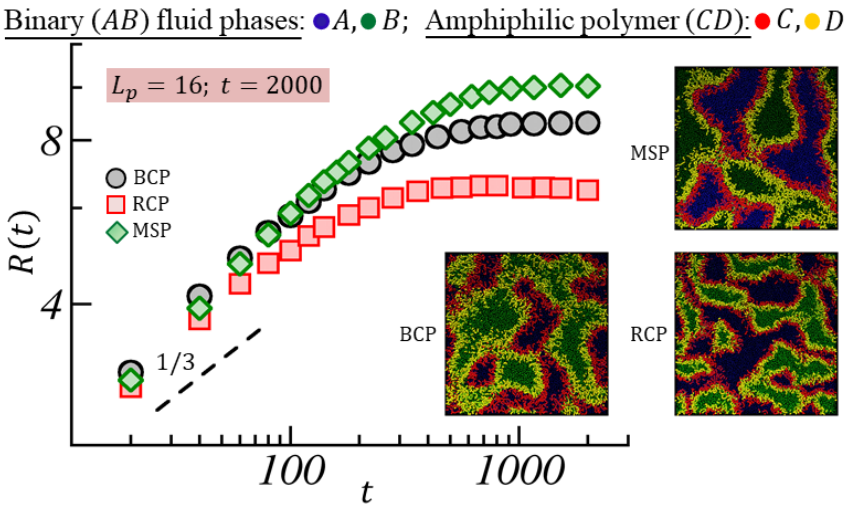


Fig. 1: Influence of amphiphilic polymers on the phase separating binary mixtures.

Continuing with this thesis, in the first chapter, we provide a detailed introduction. We discuss domain coarsening, growth laws, and the two-point equal-time correlation function as a physical observable that aligns with similar experimental measurements. The simulation modeling is explored in detail in the second chapter. In the third chapter, we investigate the phase separation dynamics of a polymeric mixture of binary (AB) simple fluid (SF) and amphiphilic polymer (AP). We examine the effects of different AP topologies, including block copolymers (BCP), ring block copolymers (RCP), and

miktoarm star polymers (MSP), on the evolution morphologies, dynamic scaling functions, and average domain size of the AB mixture. Our results demonstrate that the presence of APs leads to significantly different evolution snapshots of the SF. The deviation from dynamical scaling function is prominent for RCP. Typically, the characteristic length scale for SF follows the power law $R(t) \sim t^{\phi}$, where $\phi$ is the growth exponent. In the presence of a higher composition of AP, we notice diffusive growth ($\phi \to 1/3$) at early times, followed by saturation in length scale ($\phi \to 0$) at late time. The extent of saturation varies depending on constraints such as topologies, composition ratios, chain lengths, and chain stiffness of the APs. At lower composition ratios of APs, the system shows inertial hydrodynamic growth ($\phi \to 2/3$) at asymptotic times without a clear indication of the viscous hydrodynamic regime ($\phi \to 1$) at earlier time. Our results firmly establish the presence of hydrodynamic growth regimes in the phase separation kinetics of binary fluids influenced by low surfactant concentrations, resolving related ambiguities in $d = 3$ systems.

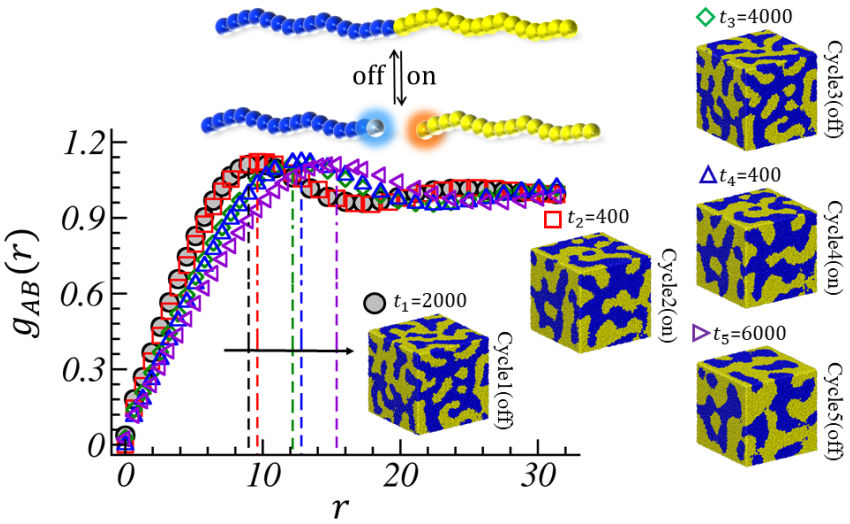


Fig. 2: Light-controlled phase-separation kinetics in BCP melts.

In the fourth chapter, we investigate the kinetic phase-separation of symmetric BCP melt in $3d$ subjected to sequential light on/off cycles. The incompatible blocks of each

BCP chain are connected by a photosensitive bond that breaks during photo-illumination (on-cycle) and recombines during the off-cycle. We establish a shorter fixed time limit for each on-cycle and focus on analyzing how the much longer time limit of the light off-cycles affects the segregation dynamics. We explore two scenarios for each off-cycle time variation: one with equal and another with increasing durations. For both cases, we determine the rate constants for bond formation and degradation reactions and assess their influence on the dynamical scaling functions and the growth scale of evolving morphologies. The average domain size typically exhibits diffusive growth ($\phi \sim 1/3$) for a couple of cycles in the beginning. However, the domain growth nearly freezes during the rest of the cycles, resulting in bicontinuous and nearly frozen isotropic morphologies.

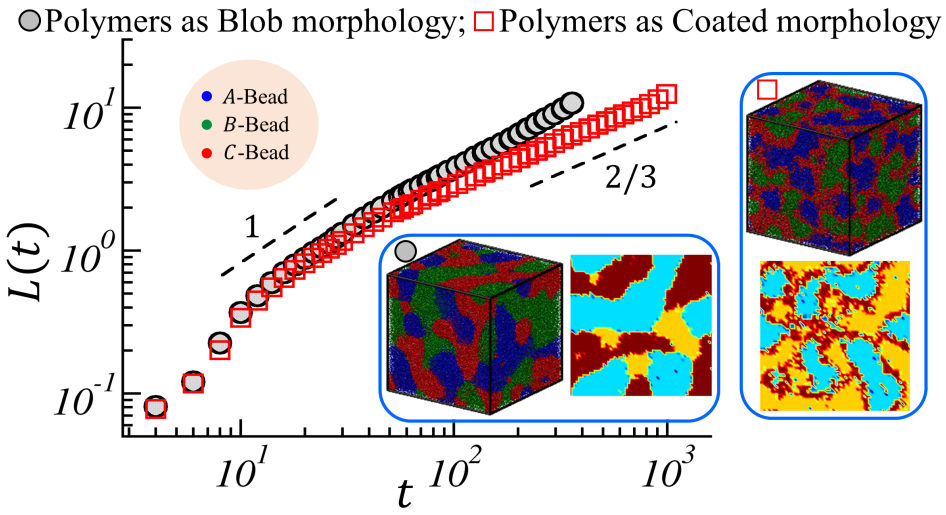


Fig. 3: Phase-segregation kinetics in simple AB fluids with polymer additives.

In the fifth chapter, we investigates the phase separation kinetics of ternary fluid mixtures consisting of two simple fluids components (A and B) and a polymeric component (C). We model the affinities between the ternary mixture components to ensure the polymeric component settles at the interface of simple fluids A and B, resulting in polymer-coated morphologies that alter the fluids' interfacial properties. This control over morphology has applications in various fields, including stabilizing emulsions and foams, rheological control, biomimetic design, and surface modification. We examine

the effects of different parameters, such as polymeric composition ratios, polymer chain rigidity and stiffness, and chain length, on the phase separation kinetics of the system. The outcomes of the simulation demonstrate that changes in the concentration of flexible polymers exhibit perfect dynamic scaling for coated topologies. The growth rate decreases due to the reduced surface tension and restricted connectivity between A- and B-rich phases with the increases in polymeric components. Variations in polymer chain rigidity at fixed composition ratios and degrees of polymerization marginally slow down the evolution kinetics of AB fluids, with the effect being more pronounced for perfectly rigid chains. Variating the chain lengths of completely rigid polymers results in a considerable variation in the length scale and dynamic scaling for the emerged coated morphologies, whereas flexible polymer chain lengths at fixed composition ratios somewhat slow down the segregation kinetics of AB fluids. The characteristic length scale follows a power-law growth, $R \sim t^{\phi}$, with a growth exponent $\phi$ that shows a crossover from the viscous ($\phi \sim 1$) to the inertial hydrodynamic ($\phi \sim 2/3$) regime.

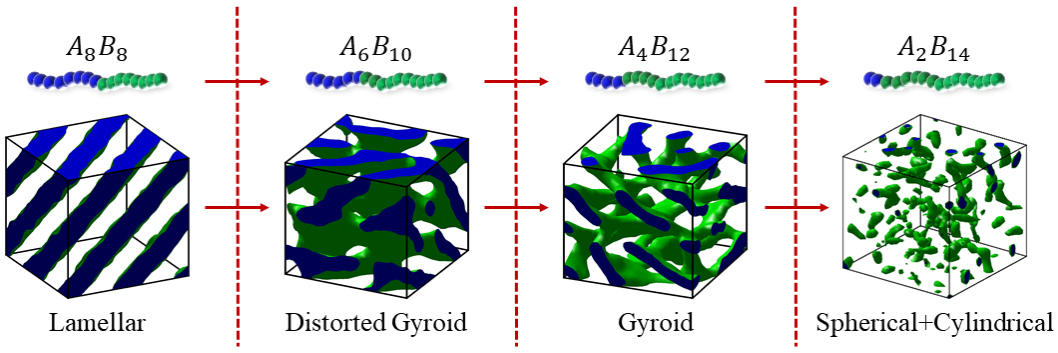


Fig. 4: Phase-separation kinetics in BCP melts system with different topologies.

In the sixth chapter, we explore the emergence of various morphologies and phase separation kinetics of distinct block copolymeric fluids using the DPD simulation method in $d = 3$. We consider three topologically different polymeric fluids to frame the kinetics and dynamical scaling functions. By varying the statistical segmental fraction values, denoted as $f$, we tune the evolution morphology. We observe that the evolution

morphologies transition from lamellae to cylindrical structures in block copolymer and miktoarm star polymer topologies when the composition ratio varies from critical (1 : 1) to highly off-critical (1 : 7). On the other hand, for ring block copolymer topology, additional evolution snapshots such as spherical structures are formed for highly off-critical compositions. The unique structure achieved is attributed to variations in the values of $f$ and the different chain topologies of the systems. To characterize these evolutionary morphologies, we analyze the radial distribution functions, radius of gyration, domain growth length, and dynamical scaling functions.